Supporting Information

Bright white-light emission from a novel donor-acceptor organic molecule in the solid state via intermolecular charge transfer

Xu-Hui Jin,[†] Cheng Chen, Cai-Xia Ren, Li-Xuan Cai and Jie Zhang*

State Key Laboratory of Structural Chemistry, Fujian Institute of Research on the Structure of Matter, CAS, Fuzhou, P. R. China, E-mail: zhangjie@fjirsm.ac.cn

[†]Present Addresses: Department of Organic Chemistry, Weizmann Institute of Science, Rehovot 76100, Israel

Table of Contents

1. Experimental details

General Information. All of the chemicals were obtained from commercial sources and used without further purification. The elemental analysis was determined using a Vario EL III CHNOS elemental analyzer. The UV-Vis absorption spectra were measured with a Perkin Elmer Lambda 900 Spectrometer. Fluorescence measurements were carried out on an Edinburgh FLS920 Luminescence Spectrometer at room temperature. The quantum yield of the crystals was measured on an FLS920 fluorescence spectrometer equipped with a $BaSO_4$-coated integrating sphere, a 450-W Xe lamp, and a R928P PMT detector using the single-photon counting mode. Scanning electron microscopy (SEM) image was recorded using a Leo Ultra 55 FEG SEM with an operating voltage of 3 keV. Cyclic voltammetry (CV) was performed using a Bio-Logic SAS (model VSP) Potentiostat/Galvanostat. All the UV-Vis absorption and fluorescence spectra in solutions were studied using pure **L-Cl·ClO$_4$** crystals. NMR measurements were carried out on a Bruker BioSpin AVANCE III spectrometer.

Synthesis

L-Cl·Cl: 4-(chloromethyl)-1-chloro-benzene (0.34 g, 2.11 mmol) was added into a solution of pyterpy (0.3 g, 0.97 mmol) in N,N-dimethylformamide (8 mL) and the reaction mixture was stirred at 125°C under N_2 for 4h. The resultant white precipitate was collected by filtration and washed with hot N,N-dimethylformamide solution, giving the production L-Cl·Cl with the yield above 50%. ^{1}H NMR (400 MHz, [D_6] DMSO): δ 9.44 (2 H, d, J 6.2), 8.90 (2 H, s), 8.80 (4 H, m), 8.70 (2 H, d, J 7.9), 8.08 (2 H, t, J 7.7), 7.69 (2 H, d, J 8.3), 7.58 (4 H, m), 6.01 (2 H, s).

^{1}H NMR

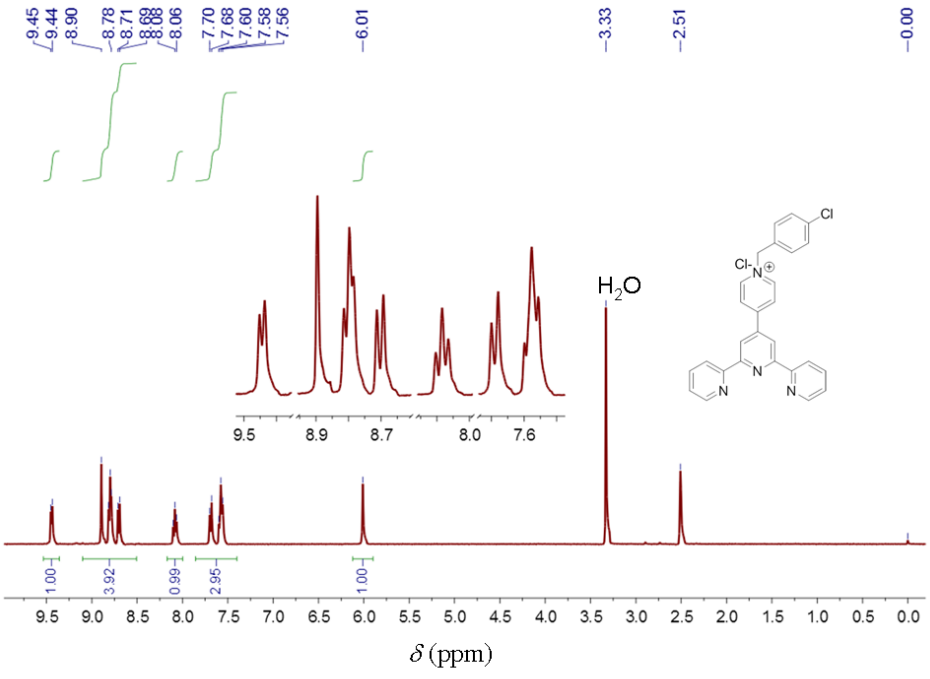

L-Cl·ClO$_4$ crystal: **L-Cl·Cl** (30 mg) was added into a solution of $LiClO_4$ (80 mg) in water (3 mL). After filtration, the filtrate was adjusted to pH 7 with 0.1M NaOH, then loaded in a Teflon autoclave and heated at 110 °C under autogenous pressure for 3 days. After the mixture was slowly cooled to room temperature within 3 days, colorless block crystals were obtained with the yield of ~45%. Calcd. for $C_{27}H_{20}N_4Cl_2O_4$: C, 60.57; H, 3.76; N, 10.46; Found: C, 60.74; H, 3.71; N, 10.48. ^{1}H NMR: (400 MHz, MeOD) δ 9.16 (2 H, d, *J* 5.4), 8.91 (2 H, s), 8.80 – 8.57 (6 H, m), 8.03 (2 H, t, *J* 6.9), 7.53 (6 H, m), 5.89 (2 H, s). ^{13}C NMR: (101 MHz, [D$_6$] DMSO) δ 156.88, 154.72, 153.85, 149.94, 145.88, 144.43, 138.23, 134.71, 133.73, 131.29, 129.71, 127.01, 125.54, 121.71, 119.38, 62.57. IR (KBr, cm^{-1}): 3122(m), 3058(m), 1641(s), 1582(s), 1545(m), 1517(m), 1495(m), 1467(m), 1392(s), 1161(m), 1089(m), 1017(m), 835(w), 793(s), 782(s), 620(s).

2. X-ray crystallographic analysis

Single crystal X-ray analysis of **L-Cl·ClO$_4$** were performed on Agilent's dual source SuperNova diffractometer by using graphite-monochromated Cu Kα (λ = 1.54178 Å) at 293(2) K. The absorption correction was performed by using the multi-scan program and the structures was solved by direct methods and refined on F^2 by full-matrix least-squares methods using the SHELXL-97 program package.

Crystal data

Crystal data for **L-Cl·ClO$_4$:** $C_{27}H_{20}C_{l2}N_4O_4$, *Mr* = 535.37, Triclinic, space group P-1, *a* = 10.0965(4), *b* = 10.8426(5), *c* = 12.8065(7) Å, α = 111.085(5)°, β = 101.692(4)°, γ = 96.127(4)°, *V* = 1255.95(10) Å^3, *Z* = 2, ρ_{calcd} = 1.416 g cm^{-3}. μ = 2.680 mm^{-1}, *F*(000) = 552, *T* = 293(2) K, 8481 reflections collected, 4945 unique (R_{int} = 0.0214). 335 refined parameters, Final residuals for 4298 reflection with $I > 2\sigma(I)$ were R_1 = 0.0702, wR_2 = 0.2095 (GOF = 1.096). CCDC 1001310.

3. Electrochemical Measurements

The cyclic voltammetry (CV) experiment of **L-Cl·ClO$_4$** was performed in dimethyl sulfoxide (DMSO) with 0.1 M tetrabutylammonium perchlorate as the electrolyte. A typical three-electrode setup was used including a Pt disk working electrode, Ag/AgCl reference electrode, and a Pt wire auxiliary electrode. Scan rates for all CV experiments were 100 mV/s. Before measurement the sample was sparged with N_2 gas for 15 min to remove oxygen. Ferrocene was used as an internal standard. Assuming ferrocene at –4.80 eV, the LUMO of **L-Cl·ClO$_4$** was calculated from their redox potentials using $-4.8 - E_{redox}$ (vs. Fc).[1] The LUMO energy of **L-Cl·ClO$_4$** measured electrochemically are consistent with the values obtained by DFT calculations.

4. Theoretical calculations

All calculations were performed using the Gaussian 09 series of programs.[2] The commonly used Becke's three parameter exchange functional combined with the LYP

correlation functional (B3LYP) was used for the calculations. The geometry of L-Cl was fully optimized by Density functional theory (DFT) calculation using the 6-31G(d) basis set (B3LYP/6-31G(d)). No symmetry constraints were applied during geometry optimization. The simulated absorption spectra and optimized excited-state geometries of L-Cl were calculated by time-dependent density functional theory (TD-DFT) at the B3LYP/6-31G(d) level. The optimized geometry of L-Cl was used for calculation of its optimized excited-state geometry. Both the optimized molecular geometry and the geometry taken from the X-ray diffraction data were used for calculations of the absorption spectra and compared. For the constrained geometry optimization of L-Cl with fixed dihedral angle θ between the terpyridine moiety and the pyridinium core, the dihedral angle between the C1–C2–C3-C4 planes in Figure S7 was fixed in the definition of the internal coordinates. L-Cl with fixed dihedral angle θ in the S_0 ground and S_1 excited state was optimized by DFT (B3LYP/6-31G(d)) and TD-DFT (B3LYP/6-31G(d)) calculation respectively. All the calculations were performed accounting for solvation effects (EtOH).

5. Additional Figures and Table

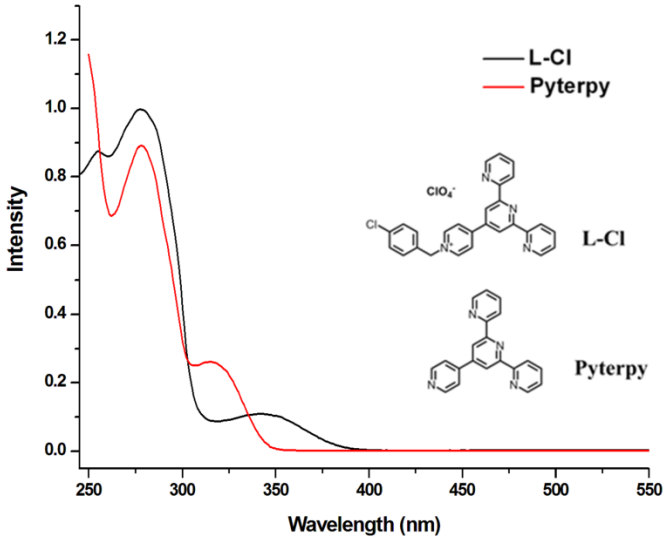

Figure S1. Absorption spectra of **L-Cl·ClO$_4$** and **pyterpy** in n-BuOH solution.

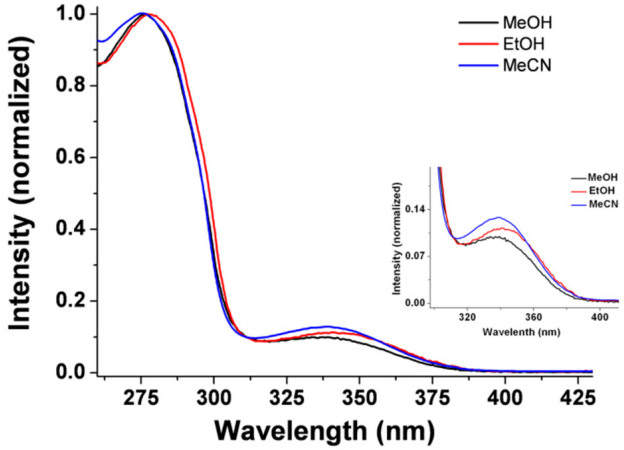

Figure S2. Absorption spectra of **L-Cl·ClO$_4$** in different solvents.

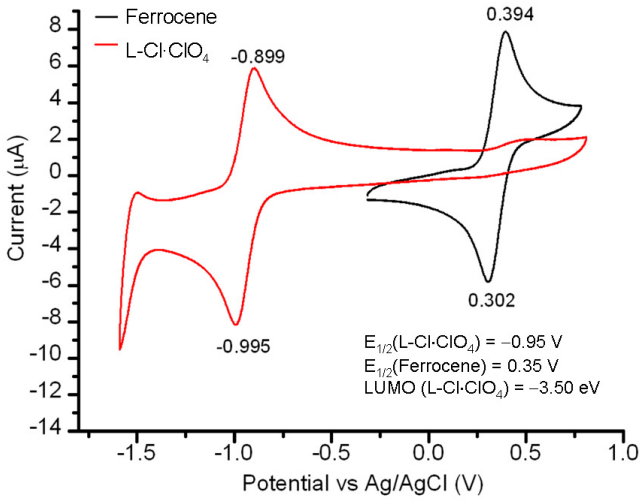

Figure S3. Cyclic voltammetry (CV) diagram of **L-Cl·ClO$_4$** in DMSO solution. CV of ferrocene is shown for the calibration. The LUMO energy is calculated as −3.50 eV.

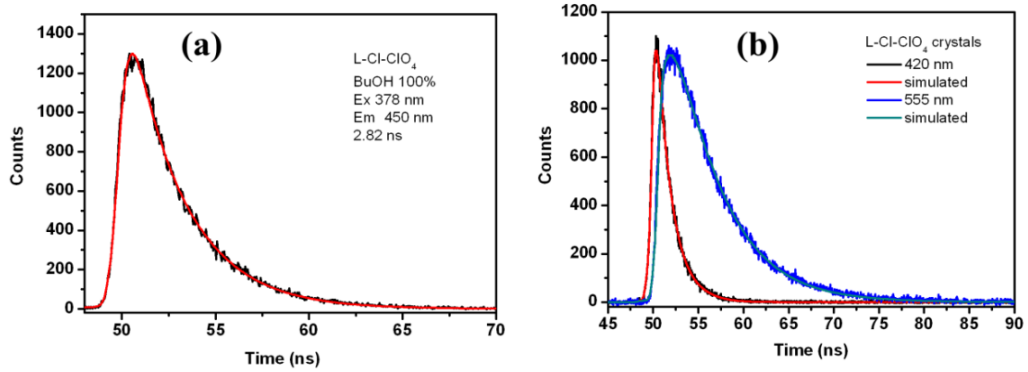

Figure S4. Photoluminescence decay of **L-Cl·ClO$_4$:** (a) in n-BuOH solution (10^{-5} M) monitored at 450 nm at 298K; (b) in crystalline state monitored at 420 nm and 555 nm respectively at 298K.

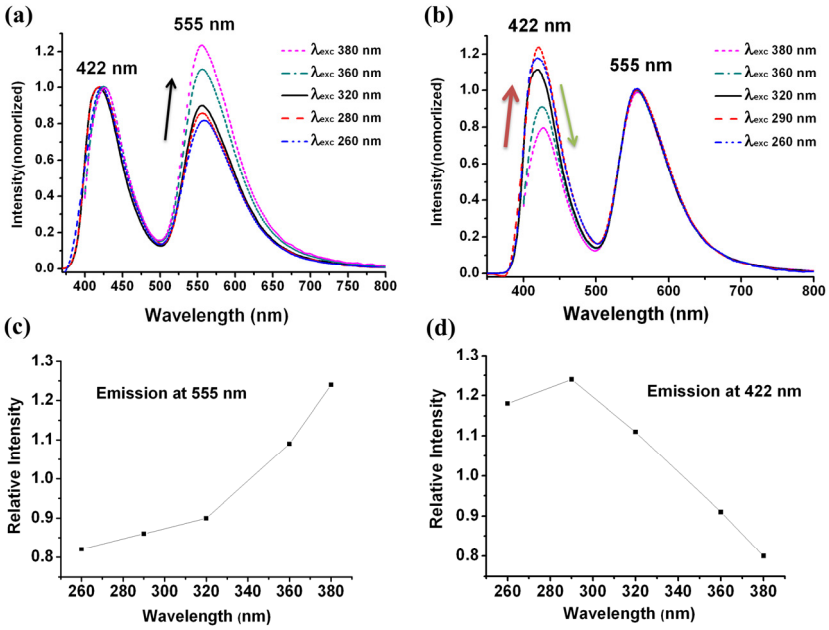

Figure S5. Emission spectra of **L-Cl·ClO$_4$** crystals under various excitation wavelengths from 260 toward 380 nm: (a) spectra with normalized intensity of the

high-energy emission with λ_{max} = 422 nm; (b) spectra with normalized intensity of the low-energy emission with λ_{max} = 555 nm; (c) the variations of the relative intensity of the low-energy emission with λ_{max} = 555 nm versus excitation wavelength; (d) the variations of the relative intensity of the high-energy emission with λ_{max} = 422 nm versus excitation wavelength.

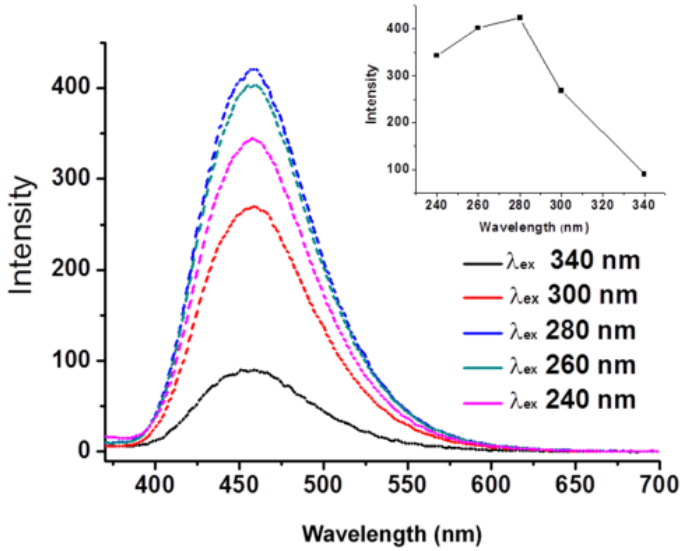

Figure S6. Fluorescence spectral changes of **L-Cl·ClO$_4$** in EtOH solution with increasing excitation wavelengths. Insert: intensity of the emission versus excitation wavelength.

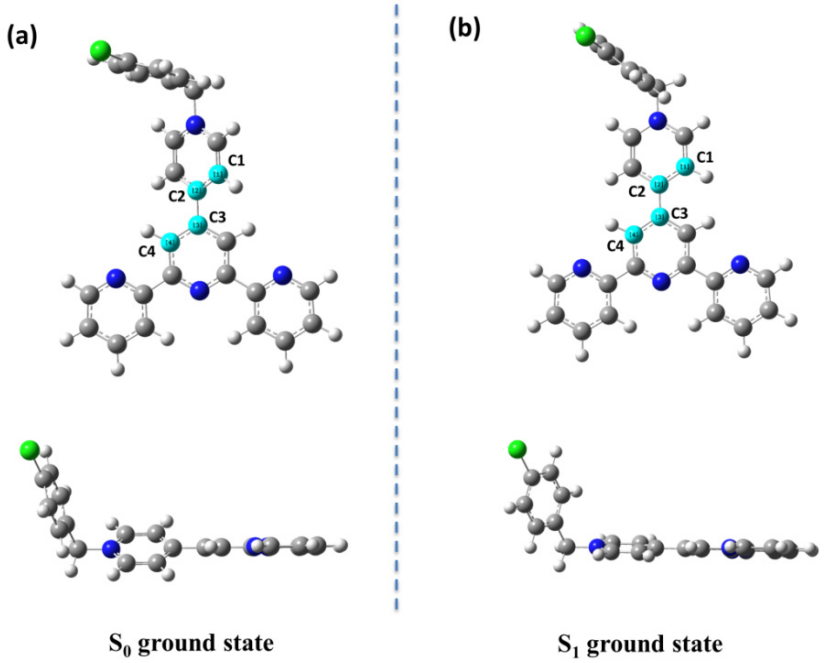

Figure S7. Optimized molecular geometries of **L-Cl** in the S_0 ground state (a) and S_1 excited state (b). The terpyridine moieties of **L-Cl** are coplanar in both the S_0 ground state and S_1 excited state.

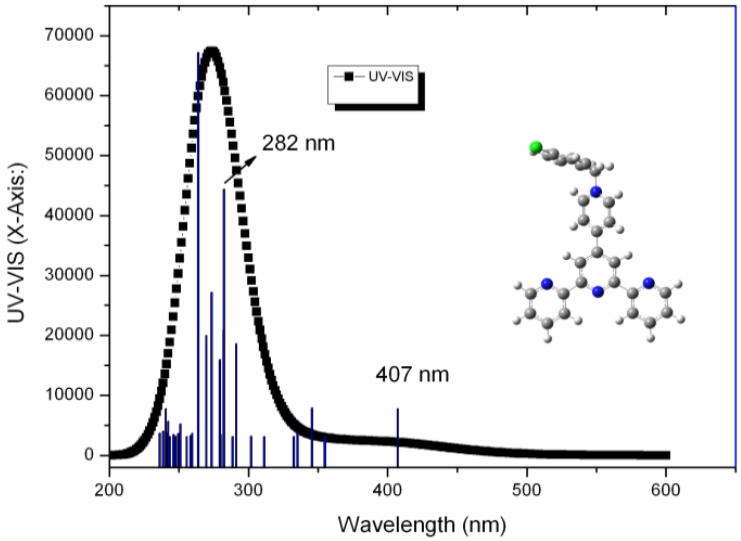

Figure S8. Calculated UV-Vis spectrum of **L-Cl** monomer at the B3LYP/6-31G (d) level using the optimized molecular geometry. Oscillator strengths: f_{407nm}/f_{282nm}=**0.113**.

Excited State 1: Singlet-A 3.0438 eV 407.33 nm f=0.0456 <S2>=0.000**

113 ->114 0.70323

113 (HOMO)	114 (LUMO)
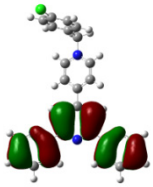	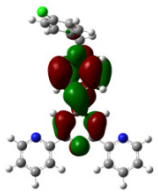

Excited State 10: Singlet-A 4.3904 eV 282.40 nm f=0.4018 <S2>=0.000**

104 ->114 -0.23531
106 ->114 -0.29526
113 ->115 0.25223
113 ->116 0.48486
113 ->117 -0.19131

113 (HOMO)	116 (LUMO+2)
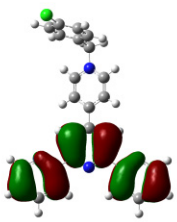	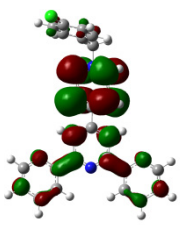

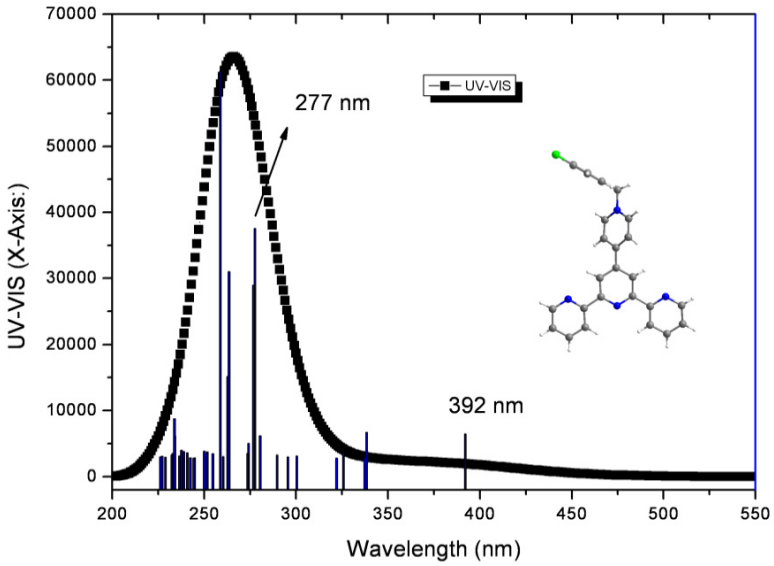

Figure S9. Calculated UV-Vis spectrum of **L-Cl** monomer at the B3LYP/6-31G (d) level using the crystal geometry. Oscillator strengths: f_{392nm} / f_{277nm} **=0.107.**

Excited State 1: Singlet-A 3.1623 eV 392.07 nm f=0.0386 <S2>=0.000**

113 ->114 0.70335

113 (HOMO)	**114 (LUMO)**
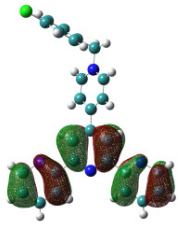	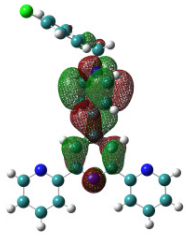

Excited State 10: Singlet-A 4.4676 eV 277.52 nm f=0.3623 <S2>=0.000**

104 ->114 0.12503

106 ->114 0.16866

110 ->115 -0.10596

110 ->116 0.18605

113 ->115 -0.17151

113 ->116 0.47272

113 ->117 -0.35211

113 (HOMO)	**116 (LUMO+2)**
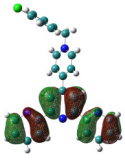	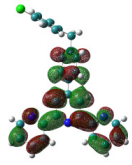

113 (HOMO)	117 (LUMO+3)
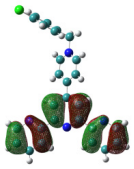	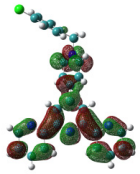

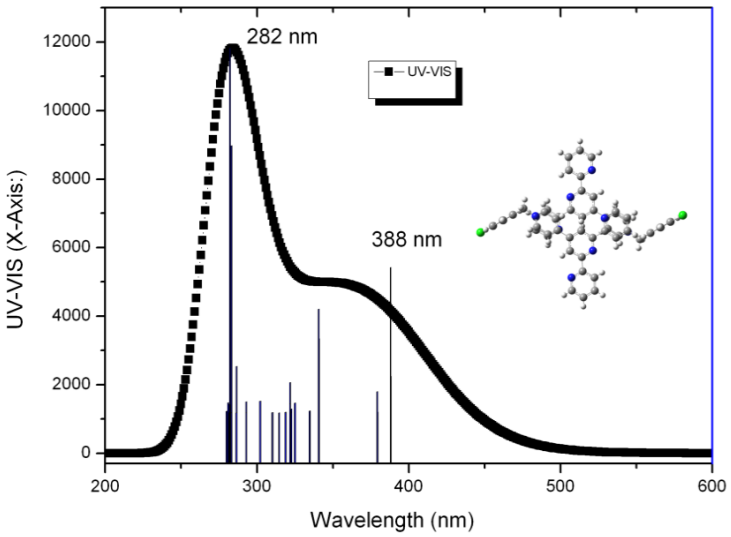

Figure S10. Calculated UV-Vis spectrum of **L-Cl** dimer at the B3LYP/6-31G(d) level using the crystal geometry. Oscillator strengths: f_{388nm}/f_{282nm}=**0.398.**

Excited State 2: Singlet-A 3.1950 eV 388.06 nm f=0.0574 <S2>=0.000**

225 -> 227	0.13763
225 -> 228	-0.27988
226 -> 227	**0.55204**
226 -> 228	-0.30350

226 (HOMO)	227 (LUMO)
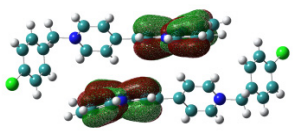	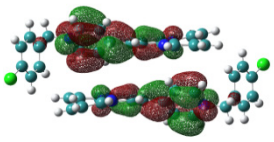

Excited State 29: Singlet-A 4.3937 eV 282.19 nm f=0.1442 <S2>=0.000**

219 -> 229	0.11806
225 -> 230	**0.31509**
225 -> 232	**-0.36295**
226 -> 229	**0.37258**
226 -> 231	-0.27425

226 (HOMO)	229 (LUMO+2)
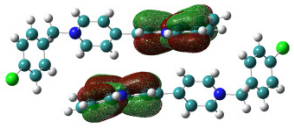	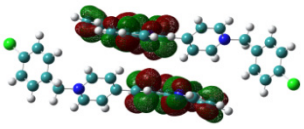
225 (HOMO-1)	**232 (LUMO+5)**
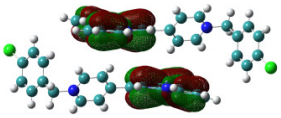	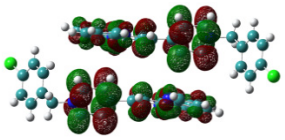
225 (HOMO-1)	**230 (LUMO+3)**
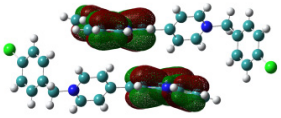	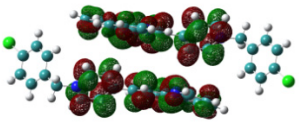

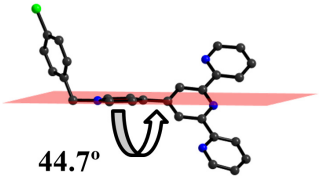

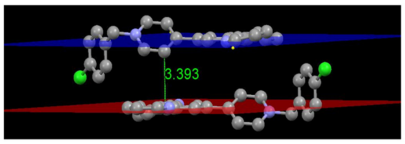

Figure S11. Molecular geometry and stacking of **L-Cl** in single crystal.

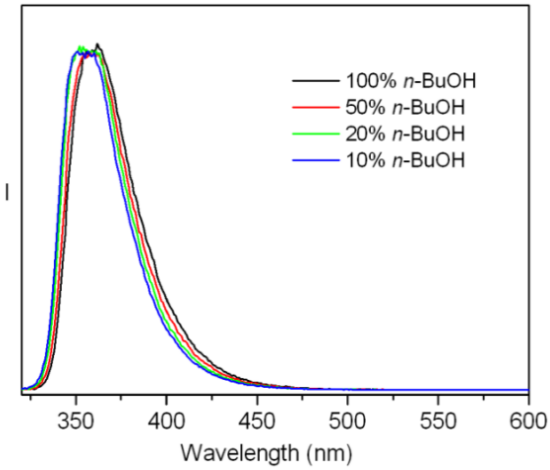

Figure S12. Normalized photoluminescence spectra of the **pyterpy** molecule in n-BuOH/ pentane mixture. No additional low-energy emission of **pyterpy** molecule was observed in its n-BuOH/ pentane mixed solution.

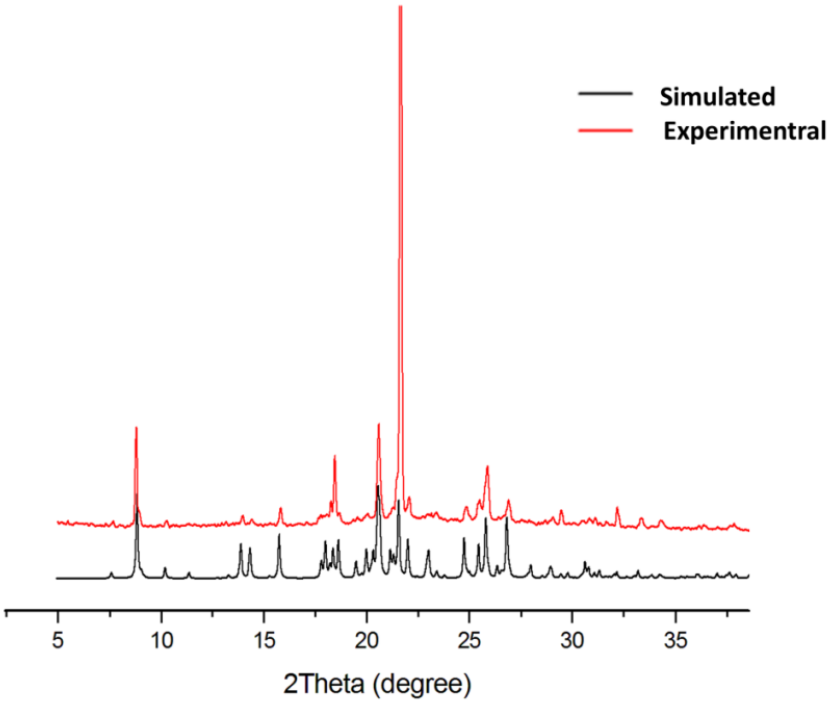

Figure S13. Simulated and experimental PXRD data of the **L-Cl·ClO$_4$** crystal.

Table S1: Values for total energy of optimized **L-Cl** with fixed dihedral angle θ between the terpyridine moiety and pyridinium ring in the S_0 ground state and S_1 excited state calculated at B3LYP/6-31G(d) level.

Twist angle	Energy in S_0 state (a.u.)	ΔE in S_0 state (kcal/mol)	Energy in S_1 state (a.u.)	ΔE in S_1 state (kcal/mol)
0	-1719.997458	1.038	-1719.896524	64.374
10	-1719.997931	0.742	-1719.896521	64.376
20	-1719.998700	0.259	-1719.896321	64.502
30	-1719.999112	0	-1719.895645	64.926
40	-1719.998954	0.099	-1719.894313	65.761
50	-1719.998279	0.424	-1719.892435	66.940

6. References

1. A. Dadvand, A. G. Moiseev, K. Sawabe, W.-H. Sun, B. Djukic, I. Chung, T. Takenobu, F. Rosei, D. F. Perepichka, *Angew. Chem. Int. Ed*. 2012, **51**, 3837.
2. Gaussian 09, Revision A.02, Frisch, M. J.; Trucks, G. W.; Schlegel, H. B.; Scuseria, G. E.; Robb, M. A.; Cheeseman, J. R.; Scalmani, G.; Barone, V.; Mennucci, B.; Petersson, G. A.; Nakatsuji, H.; Caricato, M.; Li, X.; Hratchian, H.

P.; Izmaylov, A. F.; Bloino, J.; Zheng, G.; Sonnenberg, J. L.; Hada, M.; Ehara, M.; Toyota, K.; Fukuda, R.; Hasegawa, J.; Ishida, M.; Nakajima, T.; Honda, Y.; Kitao, O.; Nakai, H.; Vreven, T.; Montgomery, J. A., Jr.; Peralta, J. E.; Ogliaro, F.; Bearpark, M.; Heyd, J. J.; Brothers, E.; Kudin, K. N.; Staroverov, V. N.; Kobayashi, R.; Normand, J.; Raghavachari, K.; Rendell, A.; Burant, J. C.; Iyengar, S. S.; Tomasi, J.; Cossi, M.; Rega, N.; Millam, J. M.; Klene, M.; Knox, J. E.; Cross, J. B.; Bakken, V.; Adamo, C.; Jaramillo, J.; Gomperts, R.; Stratmann, R. E.; Yazyev, O.; Austin, A. J.; Cammi, R.; Pomelli, C.; Ochterski, J. W.; Martin, R. L.; Morokuma, K.; Zakrzewski, V. G.; Voth, G. A.; Salvador, P.; Dannenberg, J. J.; Dapprich, S.; Daniels, A. D.; Farkas, O.; Foresman, J. B.; Ortiz, J. V.;Cioslowski, J.; Fox, D. J. Gaussian, Inc., Wallingford CT, 2009.